ELSEVIER

Journal of Biomechanics 38 (2005) 1643–1652

JOURNAL OF BIOMECHANICS

www.elsevier.com/locate/jbiomech
www.JBiomech.com

Magnetic resonance imaging for in vivo assessment of three-dimensional patellar tracking

R.A. Fellows[a], N.A. Hill[a], H.S. Gill[b], N.J. MacIntyre[a,f], M.M. Harrison[c], R.E. Ellis[d], D.R. Wilson[e,*]

[a]*Department of Medical Engineering and Human Mobility Research Centre, Queen's University, Kingston, Ont., Canada*
[b]*Nuffield Department of Orthopaedic Surgery/OOCE, Nuffield Orthopaedic Centre, University of Oxford, Oxford, UK*
[c]*Department of Surgery and Human Mobility Research Centre, Queen's University, Kingston, Ont., Canada*
[d]*School of Computing and Human Mobility Research Centre, Queen's University, Kingston, Ont., Canada*
[e]*Department of Orthopaedics, The Vancouver Hospital and Health sciences Center, University of British Columbia, Third Floor, Rm 3114, 910 West, 10th Avenue, Vancouver, BC, Canada V5Z4E3*
[f]*Department of Physical Therapy and Human Mobility Research Centre, Queen's University, Kingston, Ont., Canada*

Accepted 24 July 2004

Abstract

We have developed a non-invasive measurement technique which can ultimately be used to quantify three-dimensional patellar kinematics of human subjects for a range of static positions of loaded flexion and assessed its accuracy. Knee models obtained by segmenting and reconstructing one high-resolution scan of the knee were registered to bone outlines obtained by segmenting fast, low-resolution scans of the knee in static loaded flexion. We compared patellar tracking measurements made using the new method to measurements made using Roentgen stereophotogrammetric analysis in three cadaver knee specimens loaded through a range of flexion in a test rig. The error in patellar spin and tilt measurements was less than 1.02° and the error in lateral patellar shift was 0.88 mm. Sagittal plane scans provided more accurate final measurements of patellar spin and tilt, whereas axial plane scans provided more accurate measurements of lateral translation and patellar flexion. Halving the number of slices did not increase measurement error significantly, which suggests that scan times can be reduced without reducing accuracy significantly. The method is particularly useful for multiple measurements on the same subject because the high-resolution bone-models need only be created once; thus, the potential variability in coordinate axes assignment and model segmentation during subsequent measurements is removed.

Keywords: Knee; Patella; Kinematics; MRI; Biomechanics; Accuracy; Tracking; Patellofemoral joint

1. Introduction

Patellofemoral disorders are prevalent and serious, and many are associated with mechanical abnormalities. In a survey of people aged 25–74, 6.5% reported having experienced at least one episode of knee pain that persisted for more than 2 weeks, making it second only to neck and back as a site of pain (Praemer et al., 1992). Anterior knee pain is often associated with the eventual degeneration of the articular cartilage, which frequently leads to long-term disability (Fulkerson, 1997; Scuderi, 1995). The patella was involved in over 50% of knee osteoarthritis cases (Felson, 1990). While both anterior knee pain and arthritis are thought to have mechanical causes, these causes have not been identified because methods for assessing patellofemoral mechanics in vivo have not been available until recently.

Previous ex vivo studies of patellofemoral kinematics have revealed much about the joint, but application of these findings to patients is limited. Three-dimensional

*Corresponding author. Tel.: +1-604-875-4428; fax: +1-604-875-4376.
E-mail address: dawilson@interchange.ubc.ca (D.R. Wilson).

0021-9290/$ - see front matter © 2004 Published by Elsevier Ltd.
doi:10.1016/j.jbiomech.2004.07.021

(3D) patellofemoral kinematics have been measured in cadaver specimens loaded in mechanical rigs using a number of invasive techniques (Heegaard et al., 1994; van Kampen and Huiskes, 1990; Ahmed et al., 1999; Hsu et al., 1996). A key limitation of these ex vivo studies is that the simplified loading applied to the cadaver specimens is unlikely to simulate the in vivo loading conditions responsible for patellofemoral pain and cartilage degeneration. Morphological adaptations due to the disease process or the healing process and mechanical links to clinical symptoms such as pain and progressive cartilage degeneration cannot be studied in cadavers.

Most in vivo studies of patellar tracking have derived 2D kinematic measurements using contemporary imaging techniques. Generally, 2D images are taken of patellar position under static, and more recently dynamic (e.g., Muhle et al., 1999; Shellock et al., 1993), conditions with imaging tools such as computed tomography (CT) and magnetic resonance imaging (MRI). Patellar kinematics are usually described using 2D angles, such as the congruence angle (Muhle et al., 1999) and 2D translations or ratios, such as lateral patellar displacement (Muhle et al., 1999). It is difficult to quantify the relationship between these 2D parameters and their 3D counterparts because measurements will depend on slice position and orientation as well as patient positioning. The accuracy of these kinematic measurements is often unknown.

A few techniques have been developed to assess 3D patellar tracking in vivo. In one approach, patellofemoral kinematics were measured with markers fixed to pins driven into intracortical bone (Koh et al., 1992; Lafortune, 1984). While these measurements were accurate, the protocol is far too invasive to be practical on a larger scale. More recent techniques have employed cine-phase contrast (cine-PC) or fast-phase contrast (fast-PC) MRI (e.g., Rebmann and Sheehan, 2003) to assess 3D tracking of the loaded patellofemoral joint. Although promising, these techniques have limitations. Most notably, subjects must flex their knees through approximately 100 continuous cycles (2:48 min), limiting the magnitude of load that can be applied during testing and the applicability of this technique with subjects suffering from anterior knee pain. Motion artefacts may also be present in the images due to inconsistent movement and pulsatile motion within the imaging plane.

We have developed a new technique to measure 3D patellar kinematics in vivo that uses registration of high-resolution and low-resolution segmented magnetic resonance images. Our objective was to describe the technique and answer the following specific research questions: (1) How accurately does the method measure patellar tracking? (2) How do slice number and direction affect the method's accuracy?

2. Material and methods

Two right and one left fresh human cadaver knee specimens [all Caucasian males: age, 49.7 (26.6) years (mean (standard deviation)); height, 1.76 (0.07) m; weight, 59.74 (1.31) kg], including all tissues 45 cm proximal and distal to the joint line, were obtained from an anatomical tissue bank (ScienceCare Anatomical, Phoenix, AZ, USA). The specimens were stored frozen (at −70 °C) between experiments and thawed in air (20 h at 20 °C) prior to all preparation or testing. To prepare the cadavers for testing, the quadriceps tendon was dissected out of the musculature and a 4.8 mm diameter nylon cord was sutured to the tendon. The vastus medialis and vastus lateralis were then resected, leaving approximately 12–15 cm of exposed bone at the distal end of the femur. The exposed proximal femur was centred and rigidly fixed in a potting base made from a plastic (PVC) tube using dental cement (A-Tech Buff Special Fast Precision Stone, Ash Temple Ltd.). The potting base allowed the knees to be mounted on a loading rig (Fig. 1), on which the femur was held in a fixed, horizontal position and the tibia was allowed to hang freely. The specimens were sprayed frequently with saline solution through the course of all experiments to ensure that they did not dry out.

The knee was flexed and extended while in the rig by shortening and lengthening the cord attached to the extensor mechanism of the quadriceps tendon. The cord length could be fixed, allowing the knee to be held at static positions of flexion. The quadriceps force at each position was dictated by the weight of the tibial shank (different for each specimen) and the knee flexion angle. Thus, quadriceps loading as a function of flexion angle was consistent from experiment to experiment for each specimen (although it was not measured).

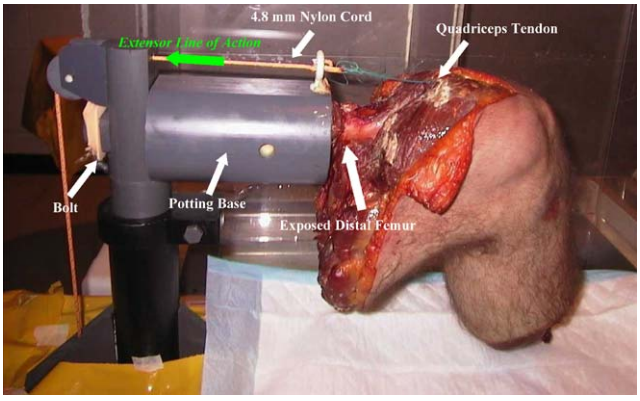

Fig. 1. MR compatible loading rig, which held the femur of the cadaver knee in a fixed and horizontal position, allowing the tibia to hang freely. The knee was flexed and extended by shortening and lengthening the cord sutured to the quadriceps tendon.

A description of the tibia, femur and patella bone surfaces was developed from a high-resolution MRI scan. Each knee was thawed and then a single high-resolution sagittal plane MRI scan (GE Signa Echo Speed Plus LX, USA) was taken of the knee in unloaded full extension. Imaging parameters were chosen in consultation with an MR technologist to maximize image resolution while restricting the overall imaging time to under 20 min and ensuring a similar field of view (FOV) for all three cadaver knees (Table 1). Bone outlines from the high-resolution scan were segmented and meshed with custom software to generate 3D geometric models (point clouds) of the femur, tibia and patella. This software has been used extensively for laboratory studies and clinical trials of computer-assisted orthopaedic surgery (Ellis et al., 1999; Croitoru et al., 2001). Coordinate systems were then assigned to each of the models.

Descriptions of the bone surfaces in loaded flexion were determined from fast, low-resolution MRI scans. The knee was fixed to the test rig with the potting base. The knee was extended by shortening the cord fixed to the quadriceps tendon. Axial and sagittal low-resolution scans of the knee were taken at sequential static positions from full extension to 45–60° of flexion (specimens 1 and 3: nine positions; specimen 2: eight positions) depending on specimen size. Imaging parameters in each plane were chosen to maximize resolution and match the FOV of the high-resolution scan while restricting the imaging time to less than 1 min (Table 2). Sagittal and axial directions were determined using accepted anatomical landmarks on localizer scans. Bony surface outlines of the tibia, patella and femur were created from each low-resolution scan by separately segmenting and extracting the bone contours (points on the bone surface), from these MR images.

The models of each bone surface were registered (shape-matched) to the data points describing their positions in loaded knee flexion using the iterative closest points (ICP) algorithm (Besl and McKay, 1992). Because a successful match using this algorithm depends on an accurate first estimate of model position, approximate alignments of models to surface outlines were found manually before registration.

At each shape-matched position of the knee, tibiofemoral and patellofemoral kinematics were found using the assigned anatomical axes and the conventions of the joint coordinate system (JCS) (Grood and Suntay, 1994). A separate coordinate system was attached to each bone model. Each system consisted of an origin and three axes: the flexion axis, directed laterally; the long axis, directed proximally; and the third axis, directed anteriorly in right knees and posteriorly in left knees. The orientation of the patella with respect to the femur was described with three clinical rotations: flexion–extension, measured as a rotation of the patella

Table 1
High-resolution MRI scan parameters used to develop the geometric model of each specimen

	Type	TE (ms)	TR (ms)	FOV (cm)	T/S (mm)	Slice no.	Matrix	NEX	Time (min)
Specimen 1	2D SE	13	540	28	2/0	47	512 × 320	3	17:19
Specimen 2	2D SE	13	490	28	2/0	43	512 × 320	3	15:43
Specimen 3	2D SE	13	640	28	2/0	47	512 × 320	3	15:29

Note: Differences in imaging time and slice number reflect the physical size differences between specimens. Imaging parameters were chosen to achieve the highest possible image resolution with a scan time under 20 min and a similar FOV for all three cadaver knees. Scan direction (sagittal) was selected using a localizer scan and by orienting the knee in the scanner. TE denotes echo time; TR denotes repetition time; FOV denotes field of view; and T/S denotes slice thickness/slice spacing.

Table 2
Low-resolution MRI scan parameters, axial and sagittal plane, used during the loading tasks for each specimen

	Direction	Type	TE (ms)	TR (ms)	FOV (cm)	T/S (mm)	Slice no.	Matrix	NEX	Time (min)
Specimen 1	Axial	2D SE	9	380	32	2/10	24	256 × 128	1	0:41
Specimen 1	Sagittal	2D SE	9	440	28	2/2	24	256 × 128	1	0:48
Specimen 2	Axial	2D SE	9	333	32	2/10	18	256 × 128	1	0:38
Specimen 2	Sagittal	2D SE	9	400	28	2/2	22	256 × 128	1	0:57
Specimen 3	Axial	2D SE	9	333	32	2/10	18	256 × 128	1	0:38
Specimen 3	Sagittal	2D SE	9	440	28	2/2	24	256 × 128	1	0:48

Note: Differences in imaging time and slice number reflect the physical size differences between specimens. Imaging parameters were chosen to achieve the highest possible image resolution and match the FOV of the high-resolution scan, while restricting imaging time to less than 1 min. Scan direction, sagittal or axial, was selected using a localizer scan and by orienting the knee in the scanner. TE denotes echo time; TR denotes repetition time; FOV denotes field of view; T/S denotes slice thickness/slice spacing; and Time denotes the time to acquire a single MR image in the 8–9 image set.

about the femoral flexion axis; medial–lateral tilt, measured as a rotation of the patella about the patellar long axis; and internal–external spin, measured as a rotation of the patella about the common perpendicular between the patellar long axis and the femoral flexion axis. The displacement of the patella with respect to the femur was described with three translations along the femoral coordinate axes: lateral patellar translation along the femoral flexion axis, proximal patellar translation along the femoral long axis and anterior patellar translation along the femoral third axis. Tibiofemoral kinematics were described in an analogous fashion to the patellofemoral system.

Spline curves were then fit to the data to provide a description of patellofemoral kinematic parameters as a function of tibiofemoral (knee) flexion. We used fourth-order uniform B-spline curves that use repeated midpoint knot insertion to minimize the effect of potentially erroneous points on the overall curve pattern by producing a line of best fit (spcrv function in the Matlab© Spline Toolbox, The Mathworks, Natick, MA, USA).

Roentgen stereophotogrammetric analysis (RSA) was used to measure patellofemoral kinematics of the same three cadaver knee specimens flexed in the same test rig. Spherical (0.8 mm diameter) tantalum beads (Tilly Medical Products, Sweden) were surgically implanted into the tibia (specimen 1: seven markers; specimens 2 and 3: eight markers), patella (specimens 1, 2 and 3: six markers) and femur (specimens 1 and 3: eight markers; specimen 2: 12 markers) of each frozen knee. A minimal amount of tissue was disrupted during the procedure. A Steinman pin was used to drill holes into the cortical layer of the frozen bone. Using a novel injection system, the tantalum beads were carefully guided through the drilled holes and placed securely into the newly created trabecular bone pockets. To verify the location of the beads in the bone after implantation, a soft-tissue CT scan (GE Light Speed, USA) of the knee was taken (FOV: 16.2 cm; T/S: 1.25/0 mm; Slice #: 120; Matrix: 512×512; time: 4:00 min). The movement of the beads within the bone marrow as a result of a complete testing and freeze/thaw cycle was investigated by repeating CT scans on one knee. The bead centres from each bone before and after were assumed to be fixed to rigid bodies, and registered to each other.

RSA measurements were made at a series of static positions throughout the flexion cycle and 3D marker positions were determined from these images using an established procedure (Alfaro-Adrian et al., 1999). After thawing, each knee was mounted in the rig and positioned in full extension. Simultaneous bi-planar X-ray images (70 KeV, 2.2 MA, film-focus: 154.2 cm) were taken of the knees and a calibration frame (Cage 21, Tilly Medical Products, Sweden) at positions of flexion ranging from full extension to 45–60° of flexion (specimens 1 and 2: nine positions; specimen 3: 10 positions). The X-rays were labelled, scanned immediately and the marker positions were digitized (Scanmaker 9600XL, Microtek, USA). We used custom RSA software to determine the 3D coordinates of the implanted beads using the scanned images and the known locations of the beads in the reference frame (Alfaro-Adrian et al., 1999).

As with the MRI procedure, accurate 3D bony surface models of the patella, tibia and femur were created by segmenting the CT scan of each knee. Coordinate systems consistent with those on the MRI models were defined for each bone (subsequently explained). From the same CT scan, the 3D locations of the centres of each RSA bead in the tibia, patella and femur in CT space were found. The CT bead locations were then registered to their corresponding RSA bead locations, and the positions of the bony surfaces and associated coordinate systems at each position of loaded flexion were determined using the transformation matrix found with the registration procedure. The registration of the CT beads to their corresponding RSA locations was run in three steps: (1) the beads were assumed to define a rigid body, and the best transformation between the two sets of points was found (Soderkvist and Wedin, 1993); (2) any potentially erroneous bead positions were found and then eliminated from each bead set; and (3) the best transformation between the two reduced sets of points was found again (Soderkvist and Wedin, 1993) and used as the final registration. This three step process was necessary because erroneous bead positions, a potential result of bead movement, could have seriously affected the accuracy of final registration between bead sets due to the low number of points being matched. Erroneous bead positions were determined in the following manner: if the distance between any two corresponding points was greater than two standard deviations above the mean distance between all beads, the bead pair was labelled as erroneous. At each knee angle, the position of the patella relative to the femur was determined as described for the MRI procedure. A spline curve was fit to these data as previously outlined.

To test the precision of our RSA procedure, we made repeated stereo radiographs on one of the cadaver specimens at 10 different flexion angles. Precision was expressed as the mean difference between patellofemoral kinematic parameters.

The coordinate axes were assigned to bone models obtained from the CT and MRI scans. First, the axes were assigned to the tibia, femur and patella surfaces determined from the CT scans (Grood and Suntay, 1994). The axes (long, third and flexion) were defined using landmarks manually chosen on a set of generic 3D femur, tibia and patella models (Table 3), in

Table 3
Anatomical landmarks used to define a set of orthogonal anatomical axes on each of the femur, tibia and patella

	Anatomical landmarks
Femur	f_1—most medial point on the medial femoral condyle f_2—most lateral point on the lateral femoral condyle f_3—intracondylar notch f_4—most proximal point in centre of femoral shaft
Tibia	t_1—most medial point on the proximal tibia t_2—most lateral point on the lateral proximal tibia t_3—most distal point in centre of tibial shaft t_4—medial tibial eminence
Patella	p_1—most medial point on mid-patella p_2—most lateral point on mid-patella p_3—most inferior point on mid-patella p_4—most superior point on mid-patella

Note: The landmarks were manually selected through visual inspection of 3D models by two observers. The chosen points were the consensus of the two observers based on the above definitions.

combination with the following equations:

$$\overrightarrow{\text{long}(n)} = \frac{\overrightarrow{n_3 n_4}}{\left\|\overrightarrow{n_3 n_4}\right\|}, \tag{1}$$

$$\overrightarrow{\text{third}(n)} = \overrightarrow{\text{long}(n)} \times \frac{\overrightarrow{n_1 n_2}}{\left\|\overrightarrow{n_1 n_2}\right\|}, \tag{2}$$

$$\overrightarrow{\text{flexion}(n)} = \overrightarrow{\text{third}(n)} \times \overrightarrow{\text{long}(n)}, \tag{3}$$

where n = femur (f), tibia (t) or patella (p).

Then, each of the three cadaver knee models was morphed using an affine transformation to the generic models so that similar and consistent anatomical landmarks and axes could be defined on all three knees.

The MRI surface models were next aligned with the CT surface models and the CT coordinate systems were assigned to the MRI models. A procedure was developed to ensure that the MR and CT coordinate systems corresponded well. This was necessary because it was difficult to segment cortical bone from MR scans. We segmented at the bone–marrow interface because cortical bone (which contains no free protons) did not display any intensity on our MRI images, making repeatable segmentation of this tissue difficult. Conversely, the intensity of the cortical bone and bone marrow on the CT scan was so similar that it was impossible to accurately differentiate between the two while segmenting. The net result of this was that the MR models were primarily of bone marrow, while the CT models contained all bone tissue, and thus the CT and MRI models of the same bone were different in shape and size. To overcome this difference in model geometry, the MRI models were first registered to the CT models using the ICP algorithm (Besl and McKay, 1992) and then these registrations were adjusted to account for the difference in tissue layers. The adjustment used an optimization algorithm to transform each of the registered patella, tibia and femur models before axes assignment, with a combination of rotations $<3^\circ$ about and translations <2 mm along the three fixed perpendicular axes of the corresponding CT models. The optimization was satisfied when the final alignment of the bones after adjustment and axes assignment produced approximately the same patellofemoral alignment values (within 0.5° and 0.5 mm) at a position of full extension (i.e., first position when loaded in the rig) for both the RSA and MRI measurement techniques. This assumption of equality between positions of extension was chosen over defining anatomical landmarks on both the CT an MRI scans because user-bias errors and differences in tissue appearance would have made it very difficult to accurately assign the same axes on CT and MRI models. Since the knees were loaded to the same starting position at full extension (using marks on the sutured cord) during both the MRI and RSA procedure, it is reasonable to assume that the patellofemoral and tibiofemoral alignment at this position are the same for both procedures.

We assessed the accuracy of our measurement technique by comparing patellar tracking measured with our MRI-based procedure to patellar tracking measured using RSA. The accuracy of each patellofemoral kinematic parameter was defined as the mean absolute difference between the corresponding RSA and MRI spline curves at 1° increments through a similar range of knee flexion. The accuracy of the kinematic measurements using both axial and sagittal plane "loaded" scans was compared. For both scan directions, the error of each kinematic parameter was found for each knee and then used to calculate a grand mean error (x_{grand}) and grand standard deviation (σ_{grand}) of that parameter across all three knees:

$$x_{\text{grand}} = \frac{1}{N}\sum_{i=1}^{k} n_i x_i, \tag{4}$$

$$\sigma_{\text{grand}} = \sqrt{\frac{1}{N-1}\sum_{i=1}^{k} n_i (x_{\text{grand}} - x_i)^2}, \tag{5}$$

$$N = \sum_{i=1}^{k} n_i, \tag{6}$$

where $i = 1, 2, \ldots, k$; k is the number of knees (three in this case), x_i the mean error for ith knee, n_i the sample size of points for calculated ith knee's mean error.

We tested the hypothesis that axial plane "loaded" scans produce lower measurement errors than sagittal plane "loaded" scans using a general linear model

ANOVA. A qualitative evaluation of the sagittal and axial low-resolution images was also performed.

The effect of the number of loaded MRI outline slices on accuracy was also explored. The full sagittal and axial "loaded" scans (Table 2) were manually reduced to simulate the effect of decreasing the slice number. Specifically, outlines describing loaded knee positions were artificially created using only every second slice, every third slice and every fourth slice in the sagittal direction, and using only every second slice and every third slice in the axial direction. This is approximately equivalent to fixing the slice thickness at 2 mm and acquiring new low-resolution scans with a slice spacing of 6, 10 and 14 mm in the sagittal direction, and of 22 and 34 mm in the axial direction. Outlines using only every fourth slice in the axial direction could not be manually produced because the patella would be described by only one slice. Slice spacing determines only the location of slices on the object being imaged, and thus will not affect the resolution of the image. The grand mean error and grand standard deviation for each patellofemoral kinematic parameter were found for each slice orientation and artificial slice number. We tested the hypothesis that low-resolution scan slice number affects procedure accuracy using a general linear model ANOVA.

3. Results

The angular precision of our RSA measurements was 0.23° in flexion, 0.11° in tilt and 0.11° in spin. The translational precision was 0.09 mm in proximal translation, 0.13 mm in lateral translation and 0.07 mm in anterior translation. The average distance between corresponding bead centres after a full testing and freeze/thaw cycle was less than 0.30 mm.

In all specimens, patterns of patellar flexion, tilt, spin and lateral translation measured using our MRI-based method were similar to those measured with RSA (Fig. 2). The mean error for all specimens through the range of flexion was less than 1.75° for measurements of attitude and less than 0.88 mm for measurements of position (Table 4).

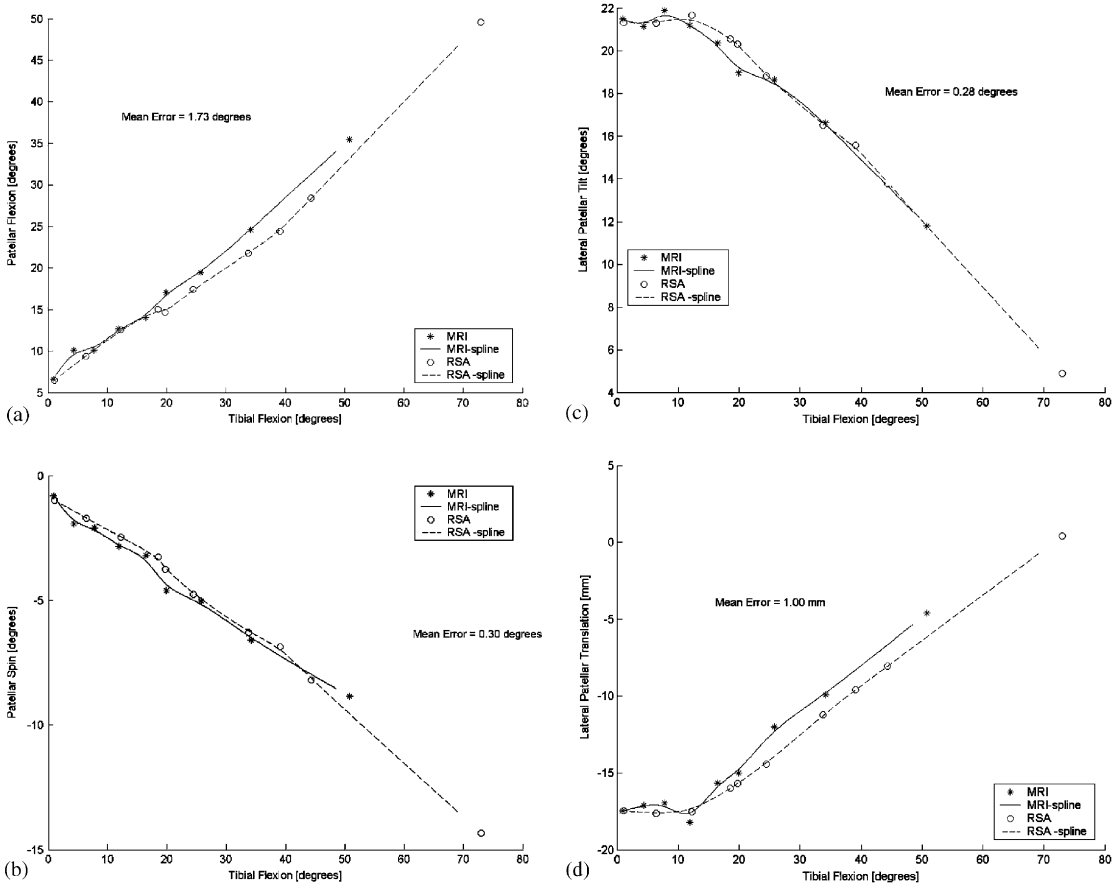

Fig. 2. Patellofemoral kinematics as a function of tibial flexion for one knee specimen measured with both our MRI-based measurement technique and RSA: (a) patellar flexion versus tibial flexion, (b) patellar spin versus tibial flexion, (c) lateral patellar tilt versus tibial flexion, (d) lateral patellar translation versus tibial flexion. The mean error between the two measurements over the flexion cycle is given on each graph.

Table 4
Overall error [grand mean (grand standard deviation)] in the MRI-based patellofemoral kinematic measurements determined using full sagittal plane loaded scans

Patellar orientation error (deg.)			Patellar translation error (mm)		
Flexion	Spin	Tilt	Proximal	Lateral	Anterior
1.75 (0.32)	1.02 (0.89)	0.30 (0.01)	0.69 (0.20)	0.88 (0.09)	0.47 (0.20)

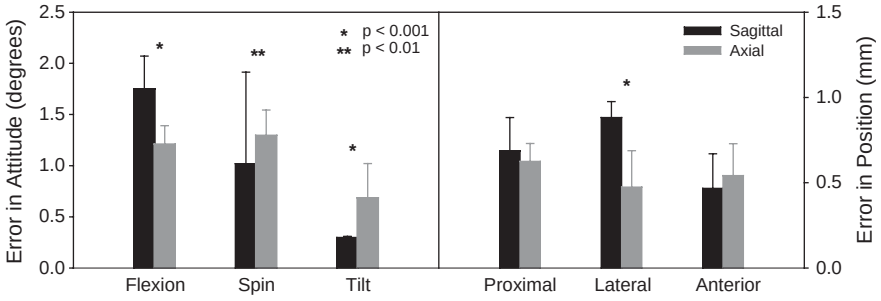

Fig. 3. Effect of loaded scan direction (axial and sagittal) on the overall mean error in the MRI-based patellar kinematic measurements. The solid columns represent the grand mean error for each kinematic parameter, and the error bars represent the grand standard deviation.

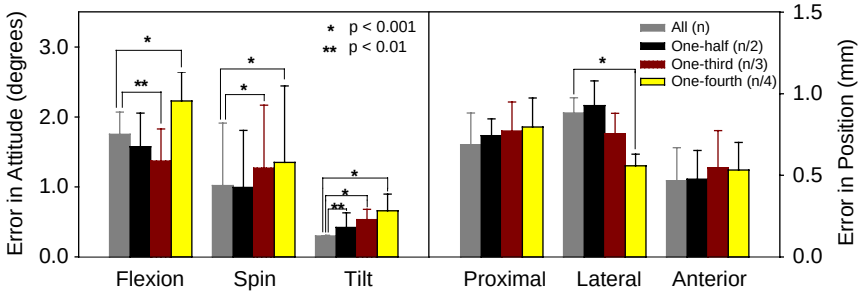

Fig. 4. Effect of the slice number in the sagittal plane loaded scan on the overall mean error in the MRI-based patellar kinematic measurements. The solid columns represent the grand mean error for each kinematic parameter, and the error bars represent the grand standard deviation.

Errors in patellar flexion and lateral translation were higher using sagittal plane "loaded" scans, while errors in patellar tilt and spin were higher using axial plane "loaded" scans (Fig. 3). We did not find a difference, for the number of knees and positions tested, between axial and sagittal plane scan errors for proximal and anterior translations.

Reducing the number of sagittal low-resolution slices had no consistent effect on the method's accuracy (Fig. 4). Reducing the number of slices by a factor of two resulted in a significantly larger error in patellar tilt measurement, but produced no significant effect on the five remaining parameters. Reducing the number of slices by a factor of three resulted in significantly higher errors in spin and tilt measurements, a significantly lower error in patellar flexion and no significant effect for lateral, proximal and anterior translation measurements. Reducing the number of slices by a factor of four resulted in significantly greater errors in all kinematic parameters, except proximal and anterior translation which were not significantly affected by slice number.

Reducing the number of axial low-resolution slices reduced the method's accuracy (Fig. 5). Reducing the number of slices by a factor of two resulted in a significantly larger error in patellar flexion, tilt, proximal translation and anterior translation, but produced no significant effect on patellar spin and lateral translation. Significantly higher errors in all parameters were found when the number of slices was reduced by a factor of three.

4. Discussion

We have developed an MRI-based method for measuring 3D patellar tracking in vivo and have assessed its accuracy by comparing patellofemoral kinematic measurements made with our novel technique

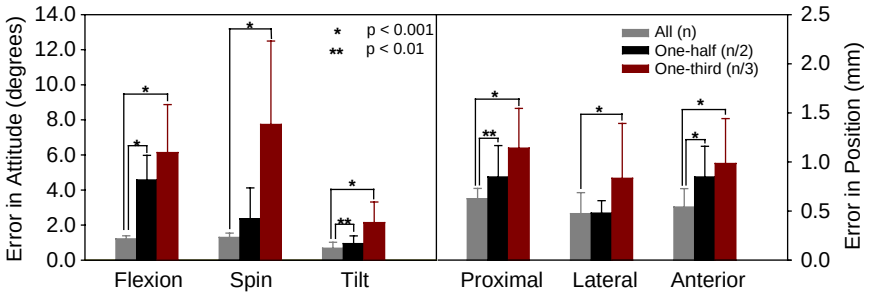

Fig. 5. Effect of slice number in the axial plane loaded scan on the overall mean error in the MRI-based patellar kinematic measurements. The solid columns represent the grand mean error for each kinematic parameter, and the error bars represent the grand standard deviation.

to those made using RSA in three cadaver knees flexed in a loading rig.

The decision about whether to use sagittal or axial plane images for the fast low-resolution loaded scans should be based on the specific measurements sought. Our results suggest that, if accurate measures of patellar spin and tilt are sought, sagittal plane images should be used. If accurate measures of lateral translation and patellar flexion are sought, axial plane images should be used. For the two imaging planes assessed in this study, measurements of rotations about an axis normal to the plane of imaging are less accurate than measurements of rotations about other axes. This may be related to how points describing the bone contours are distributed in space in the segmented images from low-resolution scans and to differences between in-plane and out-of-plane resolution in the MR scans. Proximal translation, lateral translation and patellar tilt are most often used to describe patellar tracking, but this is because these are the quantities that can be measured most directly from plain knee radiographs. Accuracy in all measurements could be optimized by taking loaded scans in both the axial and sagittal directions.

The effect of reducing data slice number on accuracy suggests that scan times for sagittal plane loaded images may be reduced while scan times for axial plane loaded images cannot be reduced without substantially decreasing accuracy. Only patellar tilt error was increased significantly by reducing the number of slices in the sagittal plane loaded scans by half. In contrast, reducing the number of axial scan slices by half significantly increased errors in all kinematic parameters except patellar spin and lateral translation. Some of these error increases, such as that for patellar flexion, were substantial. Reducing the number of slices may have reduced the error in two instances because, in those cases, specific slices from the larger set with relatively large errors may have been removed. An important implication from these findings is that MRI scan time, which is directly related to the number of slices, can be reduced with a minimal cost to the overall accuracy of the procedure if sagittal plane outlines are used. A scan time which would reduce the number of slices by a factor of two, such as 30 s, appears to be acceptable for most applications when sagittal plane outlines are used. Shorter scan times might allow subjects to apply larger loads and could potentially reduce subject fatigue and discomfort during testing.

A comparison of the accuracy of our method to that of other kinematic measurement methods is difficult because there is no standard method for defining kinematic accuracy (Crisco et al., 1999). Cine-PC MRI translation errors were 0.55 and 0.36 mm for x and y movements in the imaging plane (respectively) using a phantom, but higher for out-of-plane movements (Sheehan et al., 1998). Estimates of angular errors from Cine-PC MRI (less than 0.21°) were obtained by combining these motion phantom translation measurements and theoretical calculations (Sheehan et al., 1999). The ability of cine-PC MRI to track the 2D trajectory of a motion phantom was assessed against a reference standard (manual tracking of fiducial markers implanted into the phantom). The percentage error of the difference in the cine-PC and gold standard measurements of 2D trajectory was then used to theoretically approximate the maximum variation for a single movement of the patella by 5° about each of its three anatomic axes. Limitations to this validation approach include: (a) it does not use direct measurements of attitude; (b) movement was only created in one plane at a time, and is therefore not representative of the full 3D movement of the patellofemoral joint; (c) the phantom consisted, at least in part, of synthetic materials that may have higher contrast than the actual structure of the knee (d) it does not account for subject inconsistency in periodic knee flexion.

An advantage of our study is that we have replicated, whenever possible, the in vivo measurement procedure in our assessment of accuracy. Using cadaver knees has allowed us to incorporate the uncertainties involved in segmenting, meshing and assigning axes using MRI scans of human tissue into our accuracy assessment. These uncertainties would not have been as well incorporated if we had assessed accuracy using a phantom. A limitation of our approach is that we must rely on the CT/RSA measurements as a standard. The

repeatability of the CT/RSA measurements is superior to the accuracy measurements that we report, but it would be preferable to have measurements that are more precise because this would leave less uncertainty around the accuracy of the method.

The study's primary limitations relate to comparing the RSA and MRI measurements of tracking. The two measurements were performed on the same knees loaded in the same manner but not during the same cycle. This was because the beads required for the RSA images would distort the MRI scans. It was not possible to replicate the angles imaged during MR scanning during RSA measurement because the entire test rig (and knee) was enclosed in a transparent plastic container to protect the MR scanner from contamination and angles could not be measured reliably. Tissue was disrupted between the two measurement procedures by the bead implantation and by freezing and thawing the specimen once. Differences in patellar tracking due to these factors would most likely cause our numbers to be overestimates of the error, making them especially conservative. The assignment of anatomical axes will also have a substantial effect on our findings. Matching axis systems between the two measurement techniques was a technical challenge. The CT-based coordinate systems could not be transformed exactly to their positions in the MRI-based bone models by direct registration because different features of the bones were extracted from images acquired using different modalities. Our assumption that the coordinate systems in the MRI-based and RSA-based models coincide at one position of flexion (full extension) is reasonable. A further limitation is that we have only considered a small number of imaging parameters for our acquisition of the MRI scans. We have also neglected any motion artefact that may be present during the loading tasks in vivo. However, a study applying this method in vivo shows that the mean intrasubject variability of these measurements (three subjects, four trials) is less than 1.5° for measures of attitude and less than 1.0 mm for measures of position (Fellows et al., 2004).

Our method can be applied to study clinically relevant research questions. Axes need only be defined once for any subject no matter how many times his or her knee kinematics will be assessed, which is a particular advantage in comparisons between treatments on the same subject, such as surgery or therapy. The accuracy assessment demonstrates that this technique can measure clinically significant changes in patterns of patellar tracking. We assume, from biomechanical studies that showed that tibial tubercle realignment surgery changes patellar orientation by about 5° (Ramappa et al., 2001), that a 5° change in patellar orientation is clinically significant. This can be detected easily with our method. No additional RF coils are required to implement this method.

Our novel in vivo MRI-based technique measures 3D patellar tracking non-invasively for a range of static positions of knee flexion. The technique's accuracy is sufficient to detect clinically relevant differences in patellar tracking.

Acknowledgements

This research was supported by an Operating Grant from the Canadian Institutes of Health Research and a Strategic Grant from the Natural Sciences and Engineering Research Council. N.J. MacIntyre is supported by a Postdoctoral Fellowship from The Arthritis Society/The Canadian Institutes of Health Research, R.A. Fellows is supported by a graduate scholarship from the Natural Sciences and Engineering Research Council, and D.R. Wilson is supported by a Network Scholarship from the Canadian Arthritis Network. We thank Cyndi Harper-Little for her role in scanning the specimens, and Thomas Tang and Shawn LeClaire for their technical support and contributions.

References

Ahmed, A.M., Duncan, N.A., Tanzer, M., 1999. In vitro measurement of the tracking pattern of the human patella. Journal of Biomechanical Engineering—Transactions of the ASME 121, 222–228.

Alfaro-Adrian, J., Gill, H.S., Murray, D.W., 1999. Cement migration after THR: a comparison of Charnley Elite and Exeter femoral stems using RSA. Journal of Bone and Joint Surgery (BR) 81, 130–134.

Besl, P.J., McKay, N.D., 1992. A method for registration of 3-D shapes. IEEE Transactions on Pattern Analysis and Machine Intelligence 14, 239–255.

Crisco, J.J., McGovern, R.D., Wolfe, S.W., 1999. Noninvasive technique for measuring in vivo three-dimensional carpal bone kinematics. Journal of Orthopaedic Research 17, 96–100.

Croitoru, H., Ellis, R.E., Prihar, R., Small, C.F., Pichora, D.R., 2001. Fixation-based surgery: a new technique for distal radius osteotomy. Computer Aided Surgery 6 (3), 106–109.

Ellis, R.E., Tso, C.Y., Rudan, J.F., Harrison, M.M., 1999. A surgical planning and guidance system for high tibial osteotomy. Computer Aided Surgery 4 (5), 264–274.

Fellows, R.A., Hill, N.A., MacIntyre, N.J., Harrison, M.M., Ellis, R.E., Wilson, D.R., 2004. Repeatability of a magnetic resonance imaging-based method for measuring three-dimensional patellar kinematics in loaded flexion. 50th Meeting of the Orthopaedic Research Society.

Felson, D.T., 1990. The epidemiology of knee osteoarthritis: results from the Framingham osteoarthritis study. Seminars in Arthritis and Rheumatism 20, 42–50.

Fulkerson, J.P., 1997. Disorders of the Patellofemoral Joint. Williams and Wilkens, Baltimore, MD.

Grood, E.S., Suntay, W.J., 1994. A joint coordinate system for the clinical description of three-dimensional motions: applications to the knee. Journal of Biomechanics 105, 136–144.

Heegaard, J., Leyvraz, P., van Kampen, A., Rakotomanana, L., Rubin, P., Blankevoort, L., 1994. Influence of soft structures on

patellar three-dimensional tracking. Clinical Orthopaedics and Related Research 299, 235–243.

Hsu, H.C., Luo, Z.P., Rand, J.A., An, K.N., 1996. Influence of patellar thickness on patellar tracking and patellofemoral contact characteristics after total knee arthroplasty. The Journal of Arthroplasty 11, 69–80.

Koh, T.J., Grabiner, M.D., De Swart, R.J., 1992. In vivo tracking of the human patella. Journal of Biomechanics 25, 637–643.

Lafortune, M.A., 1984. The use of intra-cortical pins to measure the motion of the knee joint during walking. Ph.D. Thesis, Pennsylvania State University.

Muhle, C., Brossman, J., Heller, M., 1999. Kinematic CT and MR imaging of the patellofemoral joint. European Radiology 9, 508–518.

Praemer, A., Furner, S., Rice, D., 1992. Muskuloskeletal Conditions in the United States. American Academy of Orthopaedic Surgeons, Park Ridge, IL.

Ramappa, A., Wilson, D.R., Apreleva, M., Harrold, F., Fitzgibbons, P., Gill, T., 2001. The effects of medialization and anteromedialization of the tibial tubercle on patellofemoral mechanics and kinematics in knees with patellofemoral malalignment. 47th Annual Meeting of the Orthopaedic Research Society.

Rebmann, A.J., Sheehan, F.T., 2003. Precise 3D skeletal kinematics using fast phase contrast magnetic resonance imaging. Journal of Magnetic Resonance Imaging 17, 206–213.

Scuderi, G.R., 1995. The Patella. Springer, New York.

Sheehan, F.T., Zajac, F.E., Drace, J.E., 1998. Using cine phase contrast MRI to non-invasively study in vivo knee dynamics. Journal of Biomechanics 31, 21–26.

Sheehan, F.T., Zajac, F.E., Drace, J.E., 1999. In vivo tracking of the human patella using cine phase contrast magnetic resonance imaging. Journal of Biomechanical Engineering—Transactions of the ASME 121, 650–656.

Shellock, F.G., Mink, J.H., Deutsch, A.L., Foo, T.K., Sullenberger, P., 1993. Patellofemoral joint: identification of abnormalities with active-movement, ''unloaded'' versus ''loaded'' kinematic MR imaging techniques. Radiology 188, 575–578.

Soderkvist, I., Wedin, P.A., 1993. Determining the movement of the skeleton using well-configured markers. Journal of Biomechanics 26, 1473–1477.

van Kampen, A., Huiskes, R., 1990. The three-dimensional tracking pattern of the human patella. Journal of Orthopaedic Research 8, 372–382.